Springer

KSME

Journal of Mechanical Science and Technology 26 (8) (2012) 2581~2588
www.springerlink.com/content/1738-494x
DOI 10.1007/s12206-012-0638-6

Nonlinear analysis of functionally graded laminates considering piezoelectric effect †

Bashir Behjat[1,*] and Mohamad Reza Khoshravan[2]

[1]*Mechanical Engineering Faculty Sahand University of Technology Sahand New Tawn, Iran*
[2]*Mechanical Engineering Department, Tabriz University, Tabriz, Iran*

(Manuscript Received August 8, 2011; Revised January 18, 2012; Accepted March 4, 2012)

Abstract

In this paper, static bending analysis of functionally graded plates with piezoelectric layers has been carried out considering geometrical nonlinearity in different sets of mechanical and electrical loadings. Only the geometrical nonlinearity has been taken into account. The governing equations are obtained using potential energy and Hamilton's principle. The finite element model is derived based on constitutive equation of piezoelectric material accounting for coupling between elasticity and electric effect by using higher order elements. The present finite element used displacement and electric potential as nodal degrees of freedom. Results are presented for two constituent FGM plate under different mechanical boundary conditions. Numerical results for FGM plate are given in dimensionless graphical forms. Effects of material composition and boundary conditions on nonlinear response of the plate are also studied.

Keywords: Geometrically nonlinear analysis; Finite element method; Functionally graded plate; Piezoelectric layers; Static analysis

1. Introduction

Recently, the use of functionally graded materials (FGMs) has gained intensive attention in extreme high stress environment and deducing high thermal stresses. FGMs are inhomogeneous materials of which the material properties vary continuously in one or more directions. The coupled mechanical properties of FGMs caused much application in the structures. This new materials has been emerged, in which the material properties are graded but continuous throughout the thickness or any other direction [1]. This is obtained usually by gradually changing the composition of the constituent materials through the thickness. Numerous reports on a wide range of topics related to FGMs have been presented since the concept of FGMs was introduced in the analysis and modeling of such materials. Praveen and Reddy [1] presented the nonlinear static and dynamic response of functionally graded ceramic-metal plates using finite element model that accounts for Von-Karman nonlinear behavior. Yang and Shen [2] investigated nonlinear bending analysis of shear deformable FGM plates subjected to thermo-mechanical loads under various boundary conditions. They used a semi-numerical approach to calculate the nonlinear response of the FGM plate. Sundararajan et al. [3] presented the nonlinear formulation based on Von-Karman's assumptions to study the free vibration characteristics of functionally graded material (FGM) plates subjected to thermal environment. The material is assumed to be temperature dependent and Mori–Tanaka homogenization method was used. The geometrically nonlinear transient response of simply supported imperfect functionally graded plates in thermal environments is investigated by the Yang and Huang [4]. An imperfection function is used to model general forms of initial geometric. Based on the first-order shear deformation plate theory with Von-Karman non-linearity, the non-linear axisymmetric and asymmetric behavior of functionally graded circular plates under transverse mechanical loading are investigated by the Nosier and Fallah [5]. They introduced a new stress function and a potential function to obtain uncoupled equations of FG plates. Zhao and Liew studied the nonlinear response of functionally graded ceramic–metal plates and shell panels under mechanical and thermal loading [6, 7]. The nonlinear formulation is based on a modified version of Sander's nonlinear shell theory, in which the geometric nonlinearity takes the form of von Karman strains. They used element-free Kp-Ritz method to analyze the nonlinear behavior of the plates and shells. Jafari et al. [8] studied free vibration analysis of a circular FGM plate with the piezoelectric layers in top and bottom of the plate using classical plate theory. Orakdögen et al. [9] investigated the coupling effect of extension and bending in functionally graded plate subjected to transverse loading for Kirchhoff-Love plate theory equations. A nonlinear bending analysis is presented for a simply supported, functionally graded plate resting on an elastic foundation of Pasternak type by the Shen and Wang [10]. The plate is ex-

*Corresponding author. Tel.: +984123459465, Fax.: +98 412 3444309
E-mail address: behjat@sut.ac.ir
† Recommended by Associate Editor Heung Soo Kim

posed to elevated temperature and is subjected to a transverse uniform or sinusoidal load combined with initial compressive edge loads. Nie and Zhong [11] studied dynamic analysis of multi-directional functionally graded annular plates using a semi-analytical numerical method entitled the state space-based differential quadrature method. Levyakov and Kuznetsov [12] tried to construct a computationally effective curved triangular finite element for geometrically nonlinear analysis of elastic shear deformable shells fabricated from functionally graded materials. The focus is on the concise finite-element formulation under the demand of accuracy-simplicity trade-off.

Based on the coupled mechanical and electrical properties, piezoelectric structures have found much application as sensors and actuators for the purpose of monitoring and controlling the response of structures, respectively [1]. Also, piezoelectric materials have new applications for micro-electromechanical systems and intelligent material systems, especially in the medical and aerospace industries [13]. Here, some of the works that have been done in this field are mentioned.

An efficient finite element formulation based on a first-order shear deformation theory is presented for the active control of FGM plates with integrated piezoelectric sensor/actuator layers subjected to a thermal loading by the Liew et al. [13, 14]. This is accomplished using both static and dynamic piezo-thermoelastic analyses. Woo and Goo [15] presented the evaluation of a plate-type piezoelectric composite actuator with a thin sandwiched plate having four kinds of lay-up configurations by analyzing the flexural displacement. Panda and Ray [16] studied a nonlinear static finite element analysis of simply supported smart functionally graded plates in the presence/absence of the thermal environment. The substrate FG plate is integrated with the patches of piezoelectric fiber reinforced composite material. Xia and Shen [17] presented nonlinear vibration and dynamic response of FGM plates with piezoelectric fiber reinforced composite actuators. Ebrahimi et al. [18] suggested a theoretical model for geometrically nonlinear vibration analysis of piezoelectrically actuated circular plates made of functionally grade material based on Kirchhoff's-Love hypothesis with Von-Karman type geometrical large nonlinear deformations. And finally Behjat et al. [19, 20] presented the analysis of the static bending, free vibration, and dynamic response of FGPM panels and plates by finite element method. The nonlinear dynamic response and active vibration control of the piezoelectric functionally graded plate are analyzed by the Yiqi and Yiming [21].

This paper investigates the static analysis of functionally graded plates with piezoelectric layers under electrical and mechanical loadings. Geometrically nonlinear behavior of the plate has been taken into account. The analysis is carried out using nonlinear finite element method. Extensive numerical results are presented in graphical forms to give an insight into the influences of material composition and the type of loading on the nonlinear static behavior of FGM plate as an example.

Table 1. The material properties of FGM layer and piezoelectric layers used in this article [13, 24].

	Q_{11}	υ	e_{31}	e_{51}	K_{11}	K_{33}
Aluminum	70	0.3	-	-	-	-
Zirconium	151	0.3	-	-	-	-
PZT-4	74.1	0.3	-5.2	12.7	0.646×10^{-8}	0.562×10^{-8}

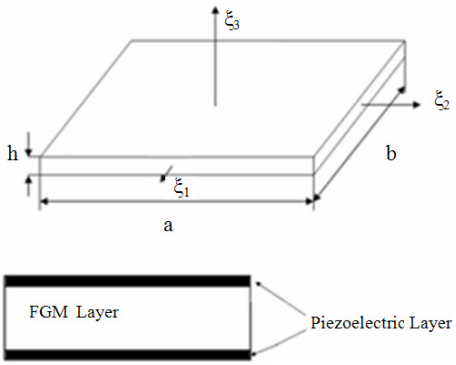

Fig. 1. Geometry and description of the FGM plate with piezoelectric layers.

2. Problem explanations

2.1 Functionally graded plates

An orthogonal coordinate system (ξ_1, ξ_2, ξ_3) is chosen such that ξ_1 and ξ_2 are lines of in plane of the neutral surface and ξ_3 defines the normal axis. The plate has the thickness h, length of a and b in each direction respectively. The functionally grading is in the thickness direction of the plate, made of two kinds of materials, the effective properties can be expressed as:

$$P_{eff}(\xi_3) = P_u V_u(\xi_3) + P_l(1 - V_u(\xi_3)) \tag{1}$$

where P_{eff} is the effective material property of the FGM plate, P_u is upper surface property of FGM plate, P_l is the lower surface property of FGM plate, and V_u is the volume fraction of the functionally gradient piezoelectric material which can be written as:

$$V_u = \left(0.5 + \frac{\xi_3}{h}\right)^n . \tag{2}$$

2.2 Geometry and material composition

In this part of paper we explain the geometry, boundary condition and materials of the functionally graded plate. The boundary conditions of the plate under current consideration is four edge simply supported (SSSS) in the first case and four edge clamped (CCCC) in the second case (Fig. 1). The piezoelectric material used in this paper is PZT-4 and the FGM layer consists of Aluminum and Zirconium and its properties are listed in Table 1. The geometry of the plate is described in

Cartesian coordinates (ξ_1, ξ_2, ξ_3) and the dimensions of the plate are defined by the same length and width of $a = b = 300$ mm and thickness of h =12 mm for functionally graded layer and h_p= 0.15 mm for each piezoelectric layer as described in Fig. 1.

3. Theoretical formulations

3.1 Piezoelectric materials constitutive relations

The constitutive relations describing the electrical and mechanical coupling for piezoelectric layers based on linear piezoelectricity theory can be expressed as [19]

$$\vec{\sigma} = \mathbf{Q}\,\vec{\varepsilon} - \mathbf{e}^T\vec{E} \tag{3}$$

$$\vec{D} = \mathbf{e}\,\vec{\varepsilon} + \mathbf{K}\,\vec{E}\,. \tag{4}$$

Here, $\vec{\sigma}$ and $\vec{\varepsilon}$ are the stress and strain tensors respectively, $\vec{D}$ is the electrical displacement vector, $E_l = -\varphi_l$ is the electrical field vector and φ is the electrical potential, **Q** is the Elasticity matrix, **e** is the piezoelectric constant matrix and **K** is the dielectric permittivity coefficient matrix. The material property gradient is assumed to be in the thickness direction base on power law distribution. The displacement-strain relations that considering the geometric nonlinear terms can be defined as:

$$\varepsilon_{ij} = \frac{1}{2}\left(\frac{\partial u_i}{\partial \xi_j} + \frac{\partial u_j}{\partial \xi_i} + \frac{\partial u_k}{\partial \xi_j}\frac{\partial u_k}{\partial \xi_i}\right). \tag{5}$$

3.2 Weak forms

The potential energy U stored in a lamina comprises the various components strain energy, piezoelectric energy and electrical energy is given by [22]

$$U = \int_V \left(\frac{1}{2}\varepsilon_{ij}\sigma_{ij} - \frac{1}{2}E_i D_i\right) dV\,. \tag{6}$$

Integrating over the element results in the weak forms of Equations [13]:

$$\int_{t_1}^{t_2}(-\delta U + \delta W_{ext})dt = 0\,. \tag{7}$$

Here, t_1 and t_2 denote two arbitrary times values and is not real time variable, so the final equations will not depend on the time necessarily, δ is the variational operator and W_{ext} is the work done by external forces. The variation of these parameters can be written as:

$$\begin{aligned}&\delta W_{ext} = \int_{0_V}\delta\vec{u}^T\vec{f_b}\,d^0V + \delta\vec{u}^T\vec{f_c} + \\ &\int_{0_s}(\delta\vec{u}^T\vec{f_s} + \delta\vec{\varphi}^T\vec{q})d^0s\end{aligned} \tag{8}$$

$$\begin{aligned}\delta U =& \int_V\Big(\delta\vec{\varepsilon}^T\left(\mathbf{Q}^{t+\Delta t}_0\vec{\varepsilon} - \mathbf{e}^{T\,t+\Delta t}_0\vec{E}\right)\Big)dv \\ &\int_V -\delta\vec{E}^T\left(\mathbf{e}^{t+\Delta t}_0\vec{\varepsilon} + \mathbf{K}^{t+\Delta t}_0\vec{E}\right)dv\end{aligned} \tag{9}$$

where $\vec{q}$ is the electrical surface charge, f_b, f_c and f_s represent the body forces, concentrated load and specified surface traction, respectively. ${}^0V$ and ${}^0S$ denote the volume and surface of the element in the first step of the analysis. To obtain the proper form of the equations, the Green-Lagrange strain tensor can be written in linear and nonlinear parts as below:

$${}_0\varepsilon_{ij} = {}_0\gamma_{ij} + {}_0\kappa_{ij} \tag{10}$$

where ${}_0\gamma_{ij}$ and ${}_0\kappa_{ij}$ are the linear and nonlinear part of the strain tensors, respectively. Substituting Eqs. (6), (8) and (10) into Eq. (7) yields the final form of the Hamilton's principle which is used to obtain the stiffness matrix of each element. The variational form of the Hamilton's principle that takes into account boundary conditions can be written as:

$$\begin{aligned}&\int_V(-\delta\vec{u}^T\rho\ddot{\vec{u}} - \delta\vec{\varepsilon}^T[Q]\vec{\varepsilon} - \delta\vec{\varepsilon}^T[e]^T\vec{E} \\ &+ \delta\vec{E}^T[e]\vec{\varepsilon} + \delta\vec{E}^T[k]\vec{E} + \delta\vec{u}^T\vec{f_b})\,dV \\ &+ \int_A(\delta\vec{u}^T\vec{f_s} + q_e\delta\phi)\,dA + \sum_{i=1}^{N}\delta\vec{u}^T\vec{f}_{pi} = 0\,.\end{aligned} \tag{11}$$

Considering Eq. (10) and doing some simplifications of the Hamilton's principle, the final form of this principle can be written as:

$$\begin{aligned}&\int_{V^0}(-\delta\vec{u}^T\rho\ddot{\vec{u}})dv + \int_{V^0}\delta\vec{e}^T\mathbf{Q}^{t+\Delta t}_0\vec{e}\,dv + \int_{V^0}\delta\vec{\eta}^T\,{}^t_0\vec{\mathbf{S}}\,dv \\ &+ \int_{V^0}\delta\vec{e}^T\,{}^t_0\vec{\mathbf{S}}\,dv + + \int_{V^0}(\delta\vec{e}^T\mathbf{e}^T({}^{t+\Delta t}_0\vec{E}) + \delta\vec{\eta}^T\mathbf{e}^T\,{}^t_0\vec{E})\,dv \\ &+ \int_{V^0}(\delta\vec{E}^T\mathbf{e}\,{}^t_0\vec{\varepsilon} + \delta\vec{E}^T\mathbf{e}\,{}^t_0\vec{e})dv + + \int_{V^0}(\delta\vec{E}^T\mathbf{K}^{t+\Delta t}_0\vec{E})\,dv \\ &+ \int_{V^0}\delta\vec{u}^T\vec{f_b}\,dV + \int_A(\delta\vec{u}^T\vec{f_s} + q_e\delta\phi)\,dA + \sum_{i=1}^{N}\delta\vec{u}^T\vec{f}_{pi} = 0\,.\end{aligned} \tag{12}$$

3.3 Finite element model

The Mindlin-Reissner plate theory is used to formulate the plate. The displacements field at the element can be defined in terms of nodal variables as follows [17]:

$$u_i = \sum_{k=1}^{q} h_k u_i^k + \frac{\xi_3}{2}\sum_{k=1}^{q} a_k h_k V_{ni}^k \tag{13}$$

where $\vec{V}_n^k$ is the unit vector in each node that is normal to the mid-surface of the element, h_k is the higher order shape function [24], $\vec{u}_i^e = \{u_{oi}, v_{oi}, w_{oi}, \alpha_i, \beta_i\}$ for i = 1, …, 16 are generalized nodal displacements and ak is the thickness of the plate in each node. The shape functions can be defined as below:

$$h_i = \frac{1}{16}(r+r_i)^2(r_0-2)(s+s_i)^2(s_0-2),\ (i=1,5,9,13)$$
$$h_i = \frac{1}{16}r_i(r+r_i)^2(1-r_0)(s+s_i)^2(s_0-2),\ (i=2,6,10,14)$$
$$h_i = \frac{1}{16}s_i(r+r_i)^2(r_0-2)(s+s_i)^2(1-s_0),\ (i=3,7,11,15)$$
$$g_{i4} = \frac{1}{16}r_i s_i(r+r_i)^2(1-r_0)(s+s_i)^2(1-s_0),\ (i=4,8,12,16) \tag{14}$$

where $r_0 = r\,r_i \quad , \quad s_0 = s\,s_i$ (15)

and s_i , r_i are the coordinate of the each node in natural coordinate system. Also the electric potential through the thickness has the linear form [19] and can be written as:

$$\varphi(r,s,\xi_3) = \sum_{i=1}^{16}\varphi_i(\xi_3)h_i(r,s) \tag{16}$$

where $\vec{\varphi}^e = \{\varphi_1, ..., \varphi_{16}\}^T$ are the nodal electric potentials in a local coordinate system. The linear and nonlinear parts of Green-Lagrange strain and the electric field vector $\vec{E}$ can be written in terms of nodal variables as:

$${}_0\gamma = \mathbf{B}_L\vec{u}^e \quad , \quad {}_0\kappa = \mathbf{B}_{NL}\vec{u}^e \quad , \quad \vec{E} = -\mathbf{B}_\varphi\vec{\varphi}^e . \tag{17a-c}$$

The B_φ , B_L and B_{NL} are matrices that relate the nodal variables with the field variables [23]. Since there are 3 layers in the plate, the integration is done for each layer separately and total stiffness element matrix is the sum of the three layers matrices. Substituting Eqs. (16) and (17) into Eq. (12) yields the final element equation as below:

$$(\mathbf{K}_L + \mathbf{K}_{NL} - \mathbf{H}_{NL})\vec{U} - \mathbf{K}_{u\varphi}\vec{\phi} = \vec{R} - {}_0^t\vec{F} - {}_0^t\vec{F}_{u\varphi} \tag{18}$$
$$\mathbf{K}_{\varphi u}\vec{U} - \mathbf{K}_{\varphi\varphi}\vec{\phi} = \vec{F}_q - {}_0^t\vec{F}_{\varphi u} - {}_0^t\vec{F}_{\varphi\varphi} \tag{19}$$

Where $\mathbf{H}_{NL}$, $\mathbf{K}_{NL}$, $\mathbf{K}_L$, $\mathbf{K}_u$ and $\mathbf{K}$ are the linear and the linear and nonlinear stiffness matrices that can be obtained from Eq. (12) and has the relations with matrices B_φ , B_L and B_{NL} as below:

$${}_0^t\mathbf{H}_{NL} = \int_{V^0} {}_0^t\mathbf{B}_{NL}\mathbf{P}\,{}_0^t\mathbf{B}_{NL}dv \tag{20}$$
$${}_0^t\mathbf{K}_{NL} = \int_{V^0} {}_0^t\mathbf{B}_{NL}\,{}_0^t\mathbf{S}\,{}_0^t\mathbf{B}_{NL}dv \tag{21}$$
$${}_0^t\mathbf{K}_L = \int_{V^0} {}_0^t\mathbf{B}_L\mathbf{Q}\,{}_0^t\mathbf{B}_L dv \tag{22}$$
$${}_0^t\mathbf{K}_{u\varphi} = \int_{V^0} {}_0^t\mathbf{B}_L\mathbf{e}\,{}_0^t\mathbf{B}_\varphi dv \tag{23}$$
$${}_0^t\mathbf{K}_{\varphi\varphi} = \int_{V^0} {}_0^t\mathbf{B}_\varphi\mathbf{K}\,{}_0^t\mathbf{B}_\varphi dv \tag{24}$$

where the matrices ${}_0^tS$ and **P** are second Piolla-Kirchhoff and electric field stiffening matrices and define as:

$$\mathbf{P} = \begin{Bmatrix} e_{13}\,{}_0^tE_3\mathbf{I}_3 & 0 & e_{15}\,{}_0^tE_1\mathbf{I}_3 \\ 0 & e_{13}\,{}_0^tE_3\mathbf{I}_3 & e_{15}\,{}_0^tE_2\mathbf{I}_3 \\ e_{15}\,{}_0^tE_1\mathbf{I}_3 & e_{15}\,{}_0^tE_2\mathbf{I}_3 & e_{15}\,{}_0^tE_3\mathbf{I}_3 \end{Bmatrix} \tag{25}$$

$${}_0^t\mathbf{S} = \begin{Bmatrix} {}_0^tS_{11}\mathbf{I}_3 & {}_0^tS_{12}\mathbf{I}_3 & {}_0^tS_{13}\mathbf{I}_3 \\ {}_0^tS_{12}\mathbf{I}_3 & {}_0^tS_{22}\mathbf{I}_3 & {}_0^tS_{23}\mathbf{I}_3 \\ {}_0^tS_{13}\mathbf{I}_3 & {}_0^tS_{23}\mathbf{I}_3 & {}_0^tS_{33}\mathbf{I}_3 \end{Bmatrix} \tag{26}$$

where I_3 is the 3×3 identity matrix and ${}_0^tS_{ij}$ is the components of the second Pioalla-Kirchhoff stress tensor in time *t*.

4. Results and discussion

The aim of this section is to apply the proposed plate element to the nonlinear static analysis of a FGM plate with the piezoelectric layers under different sets of mechanical and electrical loadings. In order to verify the accuracy and effectiveness of finite element model based on the above mentioned theory, the numerical results obtained by the present model are compared with available solutions reported in the literature. The plate under current consideration is simply supported or clamped in four edges. Also it is worth to note some points about the numerical method that is used in this paper to obtain the nonlinear response of the plate. The models are analyzed by MATLAB-R2008a software. The modified Newton-Raphson method is chosen to solve our problem and the internal energy convergence is used as convergence criteria [23]. Also 36 (6×6) rectangular elements are used to model the plate and Gauss Quadrature rule is employed for the integrations of plate in each direction. The Total Lagrangian method is used to calculate the nonlinear response of the plate.

4.1 Comparison studies

To ensure the efficiency and accuracy of the present methodology, two illustrative examples were solved for static linear analysis of FGM plates with piezoelectric layers in first example and nonlinear static response of FGM plates in the second example.

Example 1. In this example we examine the linear static response of the FGM plate with piezoelectric layers. The model under consideration is a cantilevered FGM plate consisting of

Table 2. The material properties of FGM layer and piezoelectric layers used in the example 1.

	Q_{11}	υ	d_{31}	d_{32}	K_{33}
Aluminum oxide	320.2	0.26	-	-	-
Ti-6A1-4V	105.7	0.29	-	-	-
G-1195N	63	0.3	254×10^{-12}	254×10^{-12}	0.15×10^{-8}

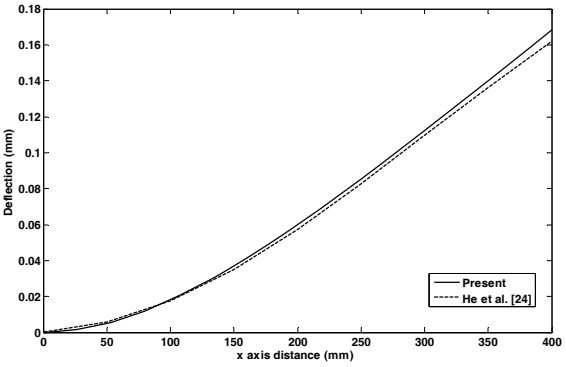

Fig. 2. Centerline deflection of the CFFF FGM plate with piezoelectric layers and comparison with Ref. [25].

combined Aluminum Oxide and Ti-6A1-4V material constituents. The piezoelectric layers consist of G-1195N in the top and bottom surfaces of the FGM plate as shown in Fig. 1. The plate is square with the same length and width of 0.4 m and thickness of 5 mm, and piezoelectric layers have thickness 0.1 mm. The material properties are given in Table 2. The static deflection of the plate with the power law exponent n = 0.5 is compared by the results reported by the He et al. [24] in the Fig. 2. As it is seen from the figure, the present results are in good agreements with the data given by the He et al. [25].

Example 2. In the second example we compare the nonlinear static response of the FGM plate. The thickness of FGM plate is 10 mm. The dimensions of the plate are defined by the length a = b = 200 mm. The panel is subjected to uniform pressure load. The plate consists of Ti–6Al–4V and Aluminum Oxide. The properties of each constituent, including Young's modulus and Poisson's ratio are listed in Table 2. The curve of static center point deflection for the FGM plate subjected to mechanical loading, for n = 0.2 and n = 0.5 is plotted in Fig. 3 and compared with the results of Zhao and Liew [7]. From these results, it can be observed that the present analysis results are in good agreements with the results of Zhao and Liew.

Example 3. In this example we examine the convergence rate of our numerical solution. To investigate such parameter, the energy convergence criterion, ε_E, [23] has been investigated in this section. Such parameter takes into account the amount of work done by the out-of balance loads on the displacement increments. This parameter defined versus out of balance forces and displacement fields as:

Table 3. Number of iterations in each load step by energy convergence criterion $\varepsilon_E = 0.01$.

Load parameter	Number of iterations	Dimensionless deflection
5	11	0.088
15	13	0.219
25	13	0.331
35	12	0.412
45	12	0.487
55	12	0.558
65	10	0.635
75	9	0.681
85	10	0.749
95	8	0.787

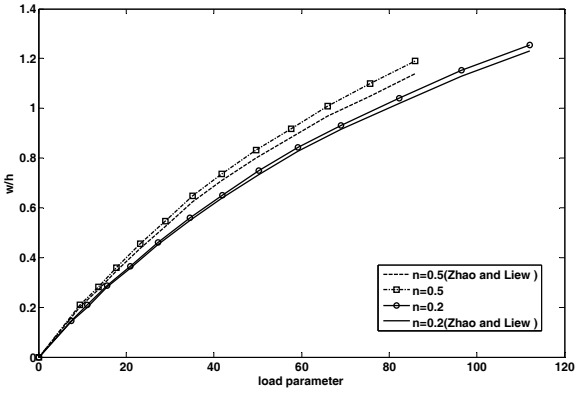

Fig. 3. Nonlinear central deflection for simply-supported Plates and comparison with the results of Zhao and Liew [7].

$$\Delta U^{(i)T}({}^{t+\Delta t}R - {}^{t+\Delta t}F^{(i-1)}) \le \varepsilon_E(\Delta U^{(1)T}({}^{t+\Delta t}R - {}^{t}F)). \quad (27)$$

In this equation, the U shows deformation vector, and superscript "i" shows the number of iteration in load step. Since this parameter contains both displacements and forces, it is in practice an attractive measure. The model under consideration is a FGM plate with piezoelectric layers. The material, geometry and boundary conditions are same as plate discussed in example 1. Table 3 shows the number of iteration in each load step that satisfies the condition ε_E = 0.01. As it is seen from Table 3, the iterations that satisfy the above mentioned condition is high in first load steps and by adding in load steps, the iterations decreases.

4.2 Mechanical loading

The FGM plate is initially subjected to mechanical loading. The boundary conditions of the plate are four edge simply supported (SSSS) and four edge clamped (CCCC) in the second case. The influence of the constituent volume fractions is studied by varying the mixing ratio of the Aluminum and Zirconia. This is carried out by varying the value of the power law exponent, n. The FGM plate is subjected to uniformly

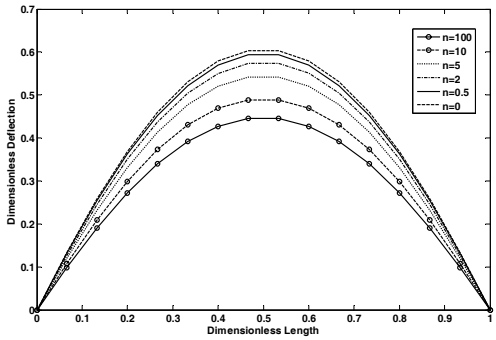

(a)

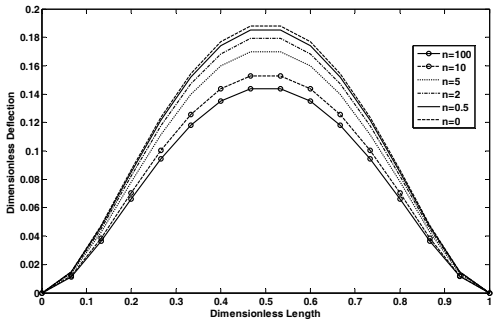

(b)

Fig. 4. Linear deflection of the plate in mechanical loading: (a) Simply supported; (b) Clamped.

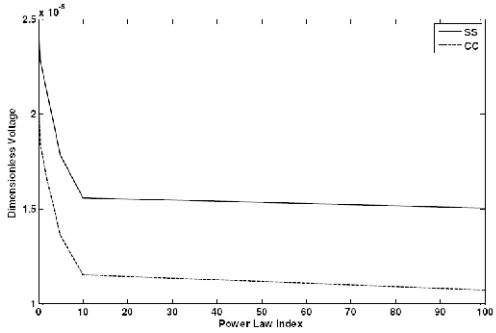

Fig. 5. Dimensionless induced voltage in linear analysis for two boundary conditions.

varying distributed load. In the first case the linear analysis of the plate has been done. The plate subjected to the uniformly distributed load q = 2 MPas. As it can be seen from the Fig. 4 by increasing the values of the n, dimensionless deflection of the plate, $\overline{w} = w/h$, decreasing. This is correct as the elastic modulus of Zirconia is higher than that of Aluminum and increasing of n leads to decrease in Aluminum constitution. Fig. 5 depicts the dimensionless maximum induced voltage, $\overline{\varphi} = \frac{\varphi k_{33}}{e_{31} h}$, in the plate in linear analysis versus power law exponent. As it can be seen from this figure, by increasing the values of n, the induced voltage in the plate is decreased. This is true because by increasing the n, the deflection in the plate decreased. Fig. 6 shows the maximum deflections of the plate

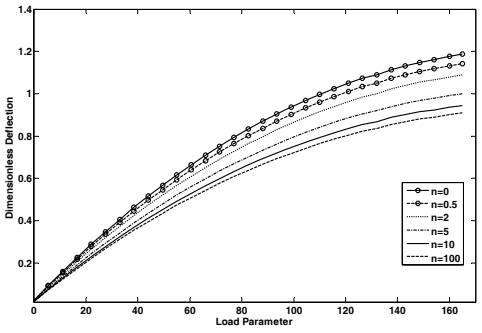

(a)

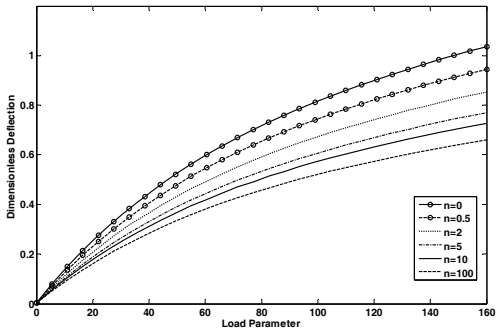

(b)

Fig. 6. Maximum deflection of the plate versus load parameter $\overline{q}$: (a) simply supported; (b) clamped.

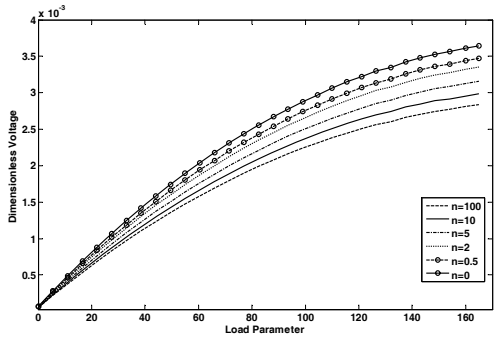

(a)

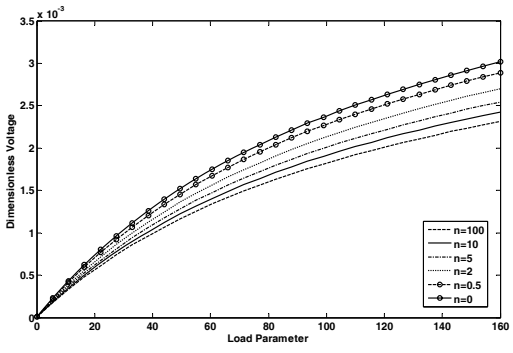

(b)

Fig. 7. Maximum voltage induced in the plate versus load parameter: (a) simply supported; (b) clamped.

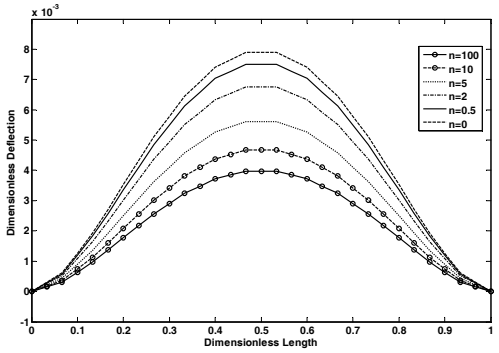

Fig. 8. Deflection of the plate under electrical loading in linear analysis.

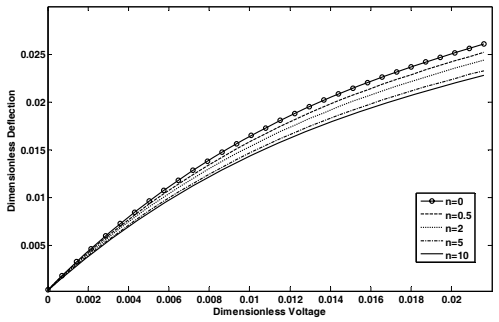

Fig. 9. The deflection of the plate under the electrical loadings for clamped boundary conditions.

versus load parameter $\overline{q} = \frac{qa^4}{E_u h^4}$ in nonlinear analysis. It can be seen that the central deflection for plates with different volume fraction exponents increases for higher values of loads. Also by increasing the load the deflection curve deviates in higher rate from the linear response. This is to be expected, because by increasing the deflection, nonlinear stiffness matrix [K_{NL}], has much influence on the response of the plate and stiffness of the plate decreases and subsequently deflection of the plate increases. Fig. 7 shows the dimensionless electric potential versus the load parameter of the plate for two boundary conditions. It can be observed that electrical potential of the piezoelectric layer generally decreases with the values of n. This is correct because by increasing the values of the n, the deflection in the plate decreases and subsequently the induced voltage in the piezoelectric layers decreases.

4.3 Electrical loading

In this section the FGM plate with piezoelectric layers is investigated by the proposed shell element under electrical loading. The plate is subjected to the uniform distributed voltage on the top piezoelectric layer of the plate. Fig. 8 shows the deflection of the plate in linear analysis for clamped boundary condition. As explained in the previous section, the deflection of the plate is decreased by increasing the power law exponent. Fig. 9 depicts the nonlinear central deflection of the lamped (CCCC) plate under the electrical loading. As explained, the central deflection for plates with different volume fraction exponents increases when the load becomes larger. The nonlinear displacement curve that corresponds to a larger volume fraction exponent deviate from linear response at a higher rate by increasing applied voltage. This is to be expected, because the stiffness of the plate becomes weaker as the volume fraction exponent increases, as explained in previous section.

5 Conclusions

The nonlinear static bending of functionally graded plates with piezoelectric layers are investigated under mechanical and electrical loadings. By using potential energy, governing differential equations are derived which takes into account the effects of piezoelectric effect and geometric nonlinearity. The results of the FGM plates with different volume fraction indexes, boundary conditions and electro-mechanical loading conditions are discussed and compared. Generally, results show that for all values of the volume fraction index n, the deflection of FGM plate increases evidently due to the applied mechanical loading. Also, by increasing the power law index, the deflection of the plate decreases for linear and nonlinear analyses. This is true because by increasing of power law index, stiffness of the plate increases and subsequently deflection of the plate decreasing. Moreover, results for electrical potential show that by increasing of volume fraction exponent, the electrical potential becomes smaller in mechanical loadings. This is true because by increasing of power law index, n, the deflection of the plate decreases and subsequently the induced voltage in the piezoelectric layers decreases.

References

[1] G. N. Praveen and J. N. Reddy, Nonlinear transient thermoelastic analysis of functionally graded ceramic-metal plates, *Int. J. Solids Struct.*, 35 (1998) 4457-4476.

[2] J. Yang and H. -S. Shen, Nonlinear bending analysis of shear deformable functionally graded plates subjected to thermo-mechanical loads under various boundary conditions, *Composites: Part B*, 34 (2003) 103-115.

[3] N. Sundararajan, T. Prakash and M. Ganapathi, Nonlinear free flexural vibrations of functionally graded rectangular and skew plates under thermal environments, *Finite Elements in Analysis and Design*, 42 (2005) 152-168.

[4] J. Yang and X. -L. Huang, Nonlinear transient response of functionally graded plates with general imperfections in thermal environments, *Comput. Methods Appl. Mech. Engrg.*, 196 (2007) 2619-2630.

[5] A. Nosier and F. Fallah, Non-linear analysis of functionally graded circular plates under asymmetric transverse loading, *Int. J. Non-Linear Mechanics*, 44 (2009) 928-942.

[6] X. Zhao and K. M. Liew, Geometrically nonlinear analysis of functionally graded shells, *Int. J. Mechanical Sciences*, 51 (2009) 131-144.

[7] X. Zhao and K. M. Liew, Geometrically nonlinear analysis of functionally graded plates using the element-free kp-Ritz

method, *Comput. Methods Appl. Mech. Engrg.*, 198 (2009) 2796-2811.

[8] S. J. Mehrabadi, M. H. Kargarnovin and M. M. Najafizadeh, Free vibration analysis of functionally graded coupled circular plate with piezoelectric layers, *Journal of Mechanical Science and Technology*, 23 (2009) 2008-2021.

[9] E. Orakdögen, S. Küçükarslan, A. Sofiyev and M. H. Omurtag, Finite element analysis of functionally graded plates for coupling effect of extension and bending, *Meccanica*, 45 (2010) 63-72.

[10] H. -S. Shen and Z. -X. Wang, Nonlinear bending of functionally garded plates subjected to combined loading and resting on elastic foundations, *Composite Structures*, 92 (2010) 2517-2524.

[11] G. Nie and Z. Zhong, Dynamic analysis of multi-directional functionally graded annular plates, *Applied Mathematical Modeling*, 34 (2010) 608-616.

[12] S. V. Levyakov and V. V. Kuznetsov, Application of triangular element invariants for geometrically nonlinear analysis of functionally graded shells, *Comput. Mech.*, DOI: 10.1007/s00466-011-0603-8.

[13] K. M. Liew, X. Q. He, T. Y. Ng and S. Sivashanker, Active control of FGM plates subjected to a temperature gradient: Modeling via finite element method based on FSDT, *Int. J. Numer. Meth. Engng.*, 52 (2001) 1253-1271.

[14] J. Yang, S. Kitipornchai and K. M. Liew, Large amplitude vibration of thermo-electro-mechanically stressed FGM laminated plates, *Comput. Methods Appl. Mech. Engrg.*, 192 (2003) 3861-3885.

[15] S. -C. Woo and N. S. Goob, Prediction of Actuating Displacement in a Piezoelectric Composite Actuator with a Thin Sandwiched PZT Plate by a Finite Element Simulation, *Journal of Mechanical Science and Technology*, 21 (2007) 455-464.

[16] S. Panda and M. C. Ray, Nonlinear finite element analysis of functionally graded plates integrated with patches of piezoelectric fiber reinforced composite, *Finite Elements in Analysis and Design*, 44 (2008) 493–504.

[17] X. -K. Xia and H. -S. Shen, Nonlinear vibration and dynamic response of FGM plates with piezoelectric fiber reinforced composite actuators, *Composite Structures,* 90 (2009) 254-262.

[18] F. Ebrahimi, M. H. Naei and A. Rastgoo, Geometrically nonlinear vibration analysis of piezoelectrically actuated FGM plate with an initial large deformation, *Journal of Mechanical Science and Technology*, 23 (2009) 2107-2124.

[19] B. Behjat, M. Salehi, M. Sadighi, A. Armin and M. Abbasi, Static, Dynamic and free vibration analysis of functionally graded piezoelectric panels using finite element method, *J. of Intelligent Material Systems and Structures*, 20 (2009) 1635-1646.

[20] B. Behjat, M. Salehi, A. Armin, M. Sadighi and M. Abbasi, Static and dynamic analysis of functionally graded piezoelectric plates under mechanical and electrical loading, *Scientia Iranica Transactions B: Mechanical Engineering*, 18 (2011) 986-994.

[21] M. Yiqi and F. Yaiming, Nonlinear dynamic response and active vibration control for piezoelectric functionally graded plate, *J. of Sound and Vibration*, 329 (2010) 2015-2028.

[22] K. J. Bathe and S. Bolourchi, A geometric and material nonlinear plate and shell element, *Computers and Structures*, 11 (1980) 23-48.

[23] K. J. Bathe, *Finite Element procedures*, New Jersey: Prentic-Hall, 1996.

[24] Y. Jiashi, *An Introduction to the Theory of Piezoelectricity*, USA: Springer science, 2005.

[25] X. Q. He, T. Y. Ng, S. Sivashanker and K. M. Liew, Active control of FGM plates with integrated piezoelectric sensors and actuators, *Int. J. of Solids and structures*, 38 (2001) 1641-1655.

Bashir Behjat entered the Mechanical Engineering program at the Amirkabir University of Technology. He received his bachelor's degree, along with a major degree in Solid Mechanics in 2006. After getting as an honored student among the students of the faculty, Bashir Behjat was accepted into the master's program in the Mechanical Engineering department at Amirkabir University of Technology in 2006. After accepting as a PhD student in Tabriz University in Iran in September 2009, he continued his Ph.D in this university as a researcher in the field of Nonlinear Finite element method and FGPM Materials and now he is associate professor in the Sahnad University of Technology in Sahand, Iran.